Bioorganic & Medicinal Chemistry 18 (2010) 6865–6873

Contents lists available at ScienceDirect

Bioorganic & Medicinal Chemistry

journal homepage: www.elsevier.com/locate/bmc

Synthesis, Pim kinase inhibitory potencies and in vitro antiproliferative activities of diversely substituted pyrrolo[2,3-*a*]carbazoles

Rufine Akué-Gédu [a,b], Lionel Nauton [a,b], Vincent Théry [a,b], Jenny Bain [c], Philip Cohen [c], Fabrice Anizon [a,b,*], Pascale Moreau [a,b,*]

[a] Clermont Université, Université Blaise Pascal, SEESIB, BP10448, F-63000 Clermont-Ferrand, France
[b] CNRS, UMR 6504, SEESIB, F-63177 Aubière, France
[c] MRC Protein Phosphorylation Unit, College of Life Sciences, Sir James Black Centre, University of Dundee, Dundee, DD1 5EH Scotland, UK

ARTICLE INFO

Article history:
Received 23 March 2010
Revised 26 May 2010
Accepted 15 July 2010
Available online 19 August 2010

Keywords:
Pyrrolo[2,3-*a*]carbazoles
Kinase inhibitors
PIM inhibitors, In vitro antiproliferative activities

ABSTRACT

The synthesis of new pyrrolo[2,3-*a*]carbazole derivatives diversely substituted at the C-6 to C-9 positions is described. These compounds were tested for their kinase inhibitory potencies toward three kinases (Pim-1, Pim-2, Pim-3) as well as for their in vitro antiproliferative activities toward a human fibroblast primary culture and three human solid cancer cell lines (PC3, DU145, and PA 1). Moreover, molecular docking studies were performed to explain the enhanced inhibitory activity of the most active compound **3d**.

1. Introduction

The Pim kinases are a small sub-family of three closely related mammalian Ser/Thr protein kinases within the CAMK (calmodulin-dependent protein kinase-related) family, comprising Pim-1, -2, -3.[1] These enzymes are known to promote cell cycle progression and to inhibit apoptosis leading to tumorigenesis.[2]

Pim kinases are emerging as important mediators of cytokine signaling pathways in hematopoietic cells, and contribute to the progression of certain leukemias and solid tumors.[3] Over-expression of the *pim-1* gene in B and T cells in transgenic mice resulted in a high level of lymphoma development in these mice, confirming the oncogenic properties of Pim-1 protein. Like Pim-1, the over-expression of Pim-2 in transgenic mice predisposes the mice to the development of lymphoma. Pim-1 also appears to be important in the development of human cancers, as the *pim-1* gene maps to an area showing karyotypic abnormalities in leukemia, and the mRNA for Pim-1 has been shown to be up-regulated in prostate cancer and leukemia. The third isoform, Pim-3, which has been less well studied, has been shown to be up-regulated in Ewing's tumor cells. Moreover, over-expression of Pim-3 has been demonstrated in a mouse model of hepatocellular carcinoma.[4]

These findings have provided a strong rationale for the development of Pim kinase inhibitors as potential antitumor agents and thus, several recent reports have described inhibitors of Pim kinases.[1,5–15] Interestingly, the presence of a proline residue (Pro123) in the hinge region of Pim-1 allows only the formation of one hydrogen bond (involving Glu121 and the amino group of ATP) and so far makes the Pim kinase family unique in the way they recognize ATP and consequently ATP mimetic inhibitors.[16]

Recently, we have published the synthesis and Pim kinase inhibitory potencies of pyrrolo[2,3-*a*]carbazole derivatives, as well as the crystal structure of the most active compound of this series (**A**) in complex with Pim-1. When tested at 10 μM toward a panel of 66 kinases, compound **A** was found to be a potent inhibitor of the Pim kinase family with IC_{50} values of 0.12 μM (Pim-1), 0.51 μM (Pim-2), and 0.01 μM (Pim-3).[17]

As shown in Figure 1, compound **A** occupied the ATP binding site of Pim-1 in the structure deposited in the PDB with accession code 3JPV. However, in contrast to typical ATP mimetic inhibitors, the planar pyrrolocarbazole scaffold was inserted into the ATP binding cleft with NH groups oriented away from the hinge region, not forming hydrogen bonds with this part of the kinase. Nevertheless, noteworthy interactions were identified: the aldehyde formed a hydrogen bond with the conserved active site lysine, Lys67, and the C2–C3 region of the inhibitor formed an aromatic stacking interaction with the P-loop phenylalanine Phe49. Based on the presence of a formyl group in the structure of these compounds, the formation of a covalent bond between the inhibitor and a

* Corresponding authors. Tel.: +33 4 73 40 79 63; fax: +33 4 73 40 77 17 (P.M.); tel.: +33 4 73 40 53 64; fax: +33 4 73 40 77 17 (F.A.).
E-mail addresses: Fabrice.ANIZON@univ-bpclermont.fr (F. Anizon), Pascale.MOREAU@univ-bpclermont.fr (P. Moreau).

0968-0896/$ - see front matter © 2010 Elsevier Ltd. All rights reserved.
doi:10.1016/j.bmc.2010.07.036

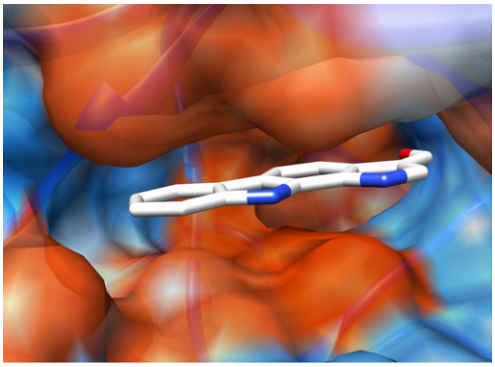

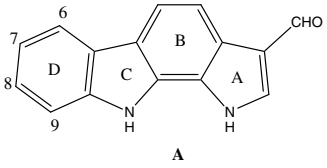

A

Figure 1. Hydrophobic surface representation of Pim-1 ATP binding site in complex with compound **A** (hydrophobic residues are colored in red and hydrophilic residues in blue). This structure was obtained from PDB 3JPV using UCSF Chimera.[22]

primary amino group of the enzyme (e.g., a Schiff base) could be envisaged. Conversely, the carbonyl group could be considered to belong to a vinylogous formamide system, with the conjugated N-1 electron pair decreasing the electrophilicity of the carbonyl group. The electron density and its distance to the lysine amino group indicated that, in the conditions used for crystallization, no covalent bond was formed between the inhibitor and the enzyme active site.

In our previous work leading to the identification of compound **A**, pyrrolo[2,3-*a*]carbazole formylated at the C-3 position was identified as a scaffold to prepare new selective Pim kinase inhibitors. In this paper, we describe the preparation of new analogues diversely substituted at the C-6 to C-9 positions. Moreover, these compounds were tested for their kinase inhibitory potencies toward the Pim kinase family (Pim-1, Pim-2, and Pim-3) as well as for their in vitro antiproliferative activities toward a human fibroblast primary culture, two human prostate cancer cell lines (PC3 and DU145) and a human ovarian teratocarcinoma cell line (PA1). Finally, molecular docking studies were performed to explain the enhanced inhibitory activity of the most active compound of this new series.

2. Chemistry

Compounds **2a–j** were synthesized in a three-step procedure from the previously described ketone **1**,[18] readily prepared in three steps from *N*-benzenesulfonylpyrrole and succinic anhydride (Fig. 2, Table 1). Compound **1** was heated in the presence of diversely substituted phenylhydrazines in the readily accessible choline chloride/zinc chloride (1:2) ionic liquid, according to the previously described procedure.[17] Subsequent oxidation with DDQ and deprotection in the presence of KOH in MeOH led to substituted pyrrolo[2,3-*a*]carbazole derivatives **2a–j**. Finally, formylation of compounds **2a–j** in Vilsmeier conditions using $POCl_3$ and DMF was performed to give the products **3a–j** in 35–85% yields (Fig. 2, Table 1). Compounds **3k** and **3l** were prepared from 2-trifluoromethylphenylhydrazine hydrochloride and ketone **1** in a 'one pot' procedure. The chemical transformation of the trifluoromethyl group to the corresponding methoxycarbonyl function likely occurred during the deprotection step. This kind of reaction has already been reported with histidine or histamine derivatives in the presence of NaOH in methanol.[19]

3. Results and discussion

The kinase inhibitory potencies of compounds **3a–l** were evaluated in duplicate as already described in the literature by Cohen's group.[20] The percentage of residual activities when the compounds were tested at 10 μM and 1 μM toward the Pim kinases (Pim-1, Pim-2, and Pim-3) are reported (Fig. 2). IC_{50} values were determined when the remaining kinase activities were less than 10% when the compounds were tested at 1 μM.

The most active compound of this series was **3d**, bearing a bromine atome in the C-6 position. Compound **3d** exhibited a high inhibitory potency toward the three Pim kinases, with IC_{50} values of 6.8 nM for Pim-1, 131 nM for Pim-2, and 12.4 nM for Pim-3. Toward Pim-2 and Pim-3, these values are in the same range as those of compound **A**. However, **3d** was found to be 17-fold more potent toward Pim-1 than compound **A**. Moreover, compounds **3f**, **3i**, **3k**, and **3l** have shown inhibitory activities in the nanomolar range toward both Pim-1 and Pim-3 kinases, whereas derivatives **3e** and **3j** inhibited Pim-3 with submicromolar IC_{50} values.

The results obtained in this structure–activity relationship studies pointed out that the introduction of substituents such as halogen atoms, methyl, cyano or nitro groups at the C-7 or C-8 positions of the heteroaromatic moiety led to less active compounds toward Pim-1 kinase.

On the contrary, the substitution of the C-6 or C-9 positions of the pyrrolo[2,3-*a*]carbazole scaffold with a bromine atom, ethyl, trifluoromethyl or methoxycarbonyl groups led to highly active compounds (**3d**, **3f**, **3i**, **3k**, **3l**), with an improvement of the inhibitory potencies toward Pim-1 when compared to compound **A**.

More particularly, compound **3d** bearing a bromine atom on the C-6 position, was the most potent derivative of this new series, and has demonstrated a modest but significant selectivity for Pim-1. To rationalize this structure–activity relationship studies, we have examined in more details the PDB 3JPV structure. As shown in Figure 3, the C-7 and C-8 positions of the D ring of the pyrrolocarbazole moiety are in close vicinity (3.51–5.04 Å) with Arg122, Pro123, and Val126 residues of the Pim-1 binding pocket. Therefore, due to steric hindrance, the substitution of these two positions seems to be detrimental to the interaction of this series of compounds with the Pim-1 kinase hinge region. On the other hand, the steric environment of the C-9 position of the D ring is much less crowded. Actually, the substitution of the C-9 position of the pyrrolocarbazole scaffold by various substituents seems to be compatible with the interaction of this series of compounds with the Pim-1 ATP binding pocket. The high inhibitory potencies of compounds **3f**, **3i**, **3k**, and **3l** bearing respectively a bromine atom, an ethyl group, a methoxycarbonyl group or a triflurometyl group at the C-9 position illustrate this structural feature.

To address the mechanism behind the highly enhanced Pim-1 inhibitory potency of compound **3d**, we have performed molecular docking studies on the interaction between the inhibitors **A**, **3d**, **3f**, **3i**, **3k**, and **3l** with the ATP binding site of Pim-1 using Sybylx1.1 (Tripos Inc., St. Louis, MO)[21] and SurFlex-Dock module. We initially

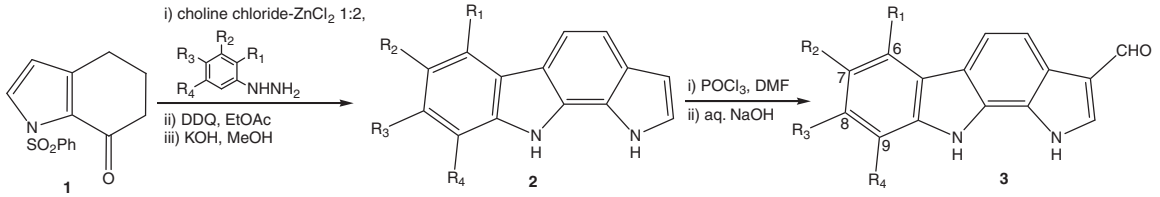

2a, **3a** $R_1 = R_3 = Cl$, $R_2 = R_4 = H$ — **2e**, **3e** $R_3 = Br$, $R_1 = R_2 = R_4 = H$ — **2i**, **3i** $R_4 = Et$, $R_1 = R_2 = R_3 = H$

2b, **3b** $R_2 = F$, $R_1 = R_3 = R_4 = H$ — **2f**, **3f** $R_4 = Br$, $R_1 = R_2 = R_3 = H$ — **2j**, **3j** $R_3 = Me$, $R_1 = R_2 = R_4 = H$

2c, **3c** $R_4 = F$, $R_1 = R_2 = R_3 = H$ — **2g**, **3g** $R_2 = NO_2$, $R_1 = R_3 = R_4 = H$ — **3k** $R_4 = CO_2Me$, $R_1 = R_2 = R_3 = H$

2d, **3d** $R_1 = Br$, $R_2 = R_3 = R_4 = H$ — **2h**, **3h** $R_2 = CN$, $R_1 = R_3 = R_4 = H$ — **3l** $R_4 = CF_3$, $R_1 = R_2 = R_3 = H$

Cpds	Kinases inhibitory potencies						Antiproliferative activities			
	Pim-1		Pim-2		Pim-3		Fibro	PA1	PC3	DU145
	10 μM	1 μM	10 μM	1 μM	10 μM	1 μM				
A[16]	2±0.4	nd (0.12±0.01)	7±1	nd (0.51±0.23)	1±5	nd (0.01±0.00)	21±1	4.5±0.4	9.5±0.5	26±2
3a	8±5	25±1	34±10	54±5	6±4	18±7	nd	nd	nd	nd
3b	4±3	15±7	21±10	84±7	5±3	12±1	nd	nd	nd	nd
3c	5±0	14±1	11±5	67±1	3±1	13±1	nd	nd	nd	nd
3d	2±0	3±2 (0.0068±0.0003)	6±2	12±2 (0.131±0.003)	5±3	10±4 (0.0124±0.0005)	1.94±0.04	<0.8	2.2±0.2	1.42±0.09
3e	44±30	56±1	39±4	37±6	15±4	8±2 (0.09±0.02)	1.13±0.05	<0.8	1.7±0.2	1.15±0.08
3f	3±2	5±1 (0.031±0.003)	28±29	40±6	9±7	6±4 (0.024±0.004)	3.4±0.2	<0.8	3.3±0.2	2.7±0.4
3g	103±35	58±6	126±12	82±4	35±10	25±3	nd	nd	nd	nd
3h	92±33	66±19	101±13	84±12	14±1	55±10	nd	nd	nd	nd
3i	1±1	7±4 (0.066±0.004)	14±1	66±10	10±5	8±3 (0.06±0.03)	5.0±0.3	1.10±0.09	8.6±0.7	5.8±0.5
3j	15±5	45±13	39±6	104±0	8±5	7±4 (0.117±0.002)	2.4±0.2	<0.8	4.1±0.4	2.5±0.1
3k	2±2	6±2 (0.030±0.004)	12±4	36±3	8±6	11±1 (0.04±0.01)	8±1	0.89±0.03	6.3±0.3	2.1±0.1
3l	1±0.3	2±0.2 (0.018±0.005)	32±12.8	56±11	1±0.9	2±0.7 (0.006±0.002)	3.24±0.32	1.96±0.19	2.99±0.45	4.47±0.21

Figure 2. Synthesis and biological activities of compounds **3a–l**. Inhibitory potencies toward Pim kinases of compounds **A** and **3a–l**: percentage of residual activities when tested at 10 μM and 1 μM (IC_{50} in μM in brackets) and antiproliferative activities (IC_{50} in μM). nd: not determined.

tried to make a docking model in accordance with the binding mode described in the co-crystal structure of Pim-1 and compound **A** (PDB code 3JPV). The first docking experiment was performed after removing the ligand and water molecules from the structure complex and adding hydrogen atoms for all amino-acid residues. Unfortunately, the docking experiment performed with this structure and compound **A** did not provide results in accordance with the binding mode described in the 3JPV structure. Actually, in the best result of this docking experiment, the ligand was located between the ATP- and phosphate-binding sites. In the best solution showing the ligand bound to the ATP pocket, the observed binding mode of **A** was different from the one described in the 3JPV structure with a flip of ~180° and a rotation of ~90° orienting the NH groups of the pyrrolocarbazole moiety toward the hinge region and the ligand carbonyl function deep inside the pocket. Thus, the formyl oxygen took the place of HOH466 making a hydrogen bond with Asp186 backbone NH. According to these results, five water molecules had to be retained in the model to get docking re-

Table 1
Chemical yields (%) for the formation of compounds **2a–j** and **3a–l**

Compds	a	b	c	d	e	f	g	h	i	j	k	l
2	88	78	55	30[a]	45[a]	68	45	56	52	65	—	—
3	47	85	71	50	60	82	35	52	50	58	9	12

[a] Compounds **2d** and **2e** were obtained simultaneously from **1** and 3-bromophenylhydrazine hydrochloride, and were separated by chromatography. Chemical yields for compounds **3k** and **3l** were calculated over four steps from ketone **1**.

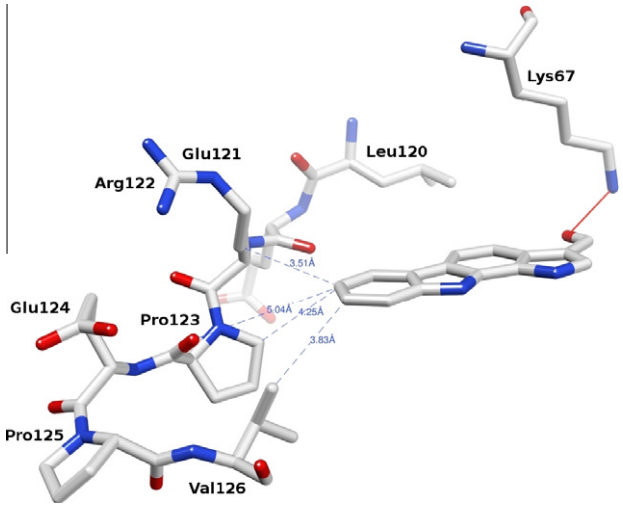

Figure 3. Interatomic distances (Å) between C-7 and C-8 positions of pyrrolocarbazole **A** and Pim-1 kinase hinge residues (PDB code 3JPV). The hydrogen bond between the formyl group and the Lys67 side chain is indicated in red line.

sults consistent with the crystallographic structure. These water molecules are HOH326, HOH466, and HOH361 that were located at the bottom of the cleft, and HOH439 and HOH360 that were situated outside of the ligand binding pocket. Thus, this model structure led to consistent results for compound **A**, as well as for compounds **3f**, **3i**, **3k**, and **3l**. In each case, a hydrogen bond was observed between the oxygen of the ligand carbonyl function and the side chain of the conserved Lys67, and NH groups were oriented away from the hinge region (Fig. 4). Additionally, the hydrogen atom at the N1 position of the ligand was hydrogen bonded with HOH360 which in turn interact with Glu171 backbone carbonyl. The interaction between HOH360 and **A** was not observed in the 3JPV structure because, in addition to water molecules HOH439 and HOH360, which were observed in the X-ray crystal structure, other water molecules are probably present in the same region as it can be deduced from the Fo–Fc map contoured at 3.5 σ which showed positive electron densities in this area. These water molecules were not set in the 3JPV structure due to an insufficient resolution (2.35 Å) and because they were not directly bonded to the protein amino-acid residues. Therefore, due to the assumed presence of this water molecule network, no direct H-bond between the hydrogen atom at the N1 position of the ligand and HOH360 could be observed in the X-ray crystal structure.

The difference of Pim-1 inhibitory potency measured between compound **A** and the most potent inhibitor **3d** could be explained by the presence of a bromine atom at the C-6 position close to the oxygen of the Glu121 backbone carbonyl. This substitution led to a repulsive effect positioning the ligand higher in the binding cleft. Consequently, either the hydrogen atom at the N-1 position or the one at the N-10 position are able to establish a hydrogen bond with HOH360, making a water bridge with Glu171 backbone carbonyl. Thus, as shown in Figure 4, the binding mode of **3d** is clearly different from the one of the other compounds examined in these docking studies. Together with the H-bond with Lys67, these interactions with HOH360 led to a stronger binding of **3d** with Pim-1, explaining the low nanomolar potency of this compound.

In vitro antiproliferative activities of compounds **3d**, **3e**, **3f**, **3i–3l**, which have shown potent inhibitory potencies against the kinases tested, were evaluated toward a human fibroblast primary culture and three human solid cancer cell lines: PA 1 (ovarian carcinoma), PC3 and DU145 (human prostate cancer cells). The antiproliferative effect (IC_{50}) of the tested compounds was assessed by the resazurin reduction test.[23] Compared with the other cell line used, PA1 cells were more sensitive to the tested compounds. The best potencies were found for compounds **3d**, **3e**, **3f**, and **3j** with IC_{50} values in 1–4 μM range for PC3, DU145 and fibroblast cell lines and submicromolar range for PA1 cell line. Compounds **3i**, **3k**, and **3l** were found to be slightly less active with IC_{50} values of 1.1 μM, 0.89 μM and 1.96 μM, respectively, toward PA1 cells and IC_{50} values in 2–8 μM range for PC3, DU145, and fibroblast cell lines. In summary, all the tested compounds have shown interesting antiproliferative activities toward the tested cell lines.

4. Conclusion

In this paper, we have described the synthesis of diversely substituted pyrrolo[2,3-*a*]carbazoles. The synthetic approach re-

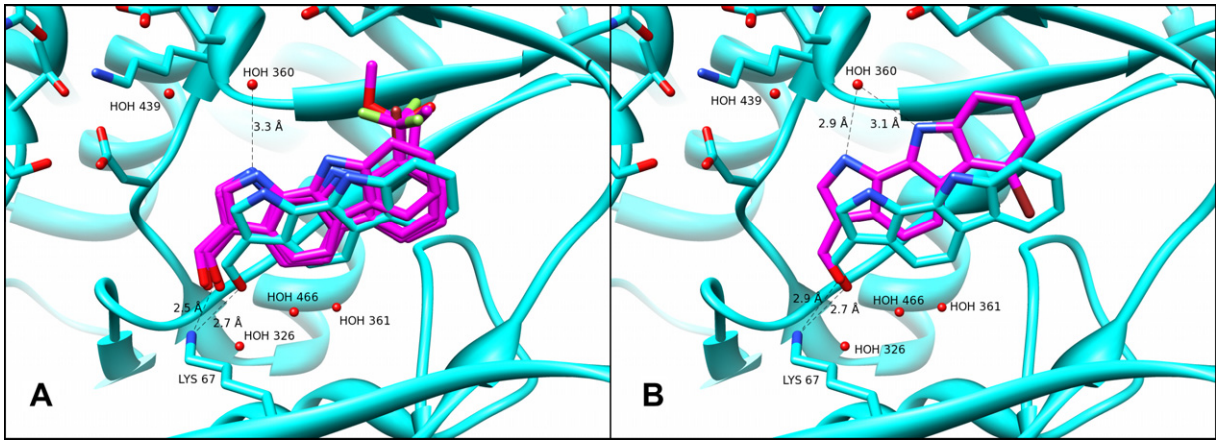

Figure 4. Docking model of compounds **A**, **3d**, **3f**, **3i**, **3k**, and **3l** into the ATP binding site of Pim-1. (A) Superimposition of compound **A** from the 3JPV structure (cyan) and compounds **A**, **3f**, **3i**, **3k**, and **3l** in the docking model (purple). (B) Superimposition of **A** from the 3JPV structure (cyan) and compound **3d** in the docking model (purple). Hydrogen bonds are indicated in broken black lines. The length indicated for H-bonds between compounds **3f**, **3i**, **3k**, and **3l** and Lys67/HOH360 are mean values.

ported here allows the substitution of the heteroaromatic ring in the C-6, C-7, C-8, C-9 positions by either electron donor or acceptor substituents. Compound **3d**, bearing a bromine atom at the C-6 position was found to be the most potent inhibitor of the series toward Pim kinases, with a 17-fold higher activity toward Pim-1 than compound **A**. Moreover, when compared to compound **A**, the newly synthetised compounds **3d**, **3e**, **3f**, and **3i–3l** that have demonstrated kinase inhibitory potencies have also shown increased potent antiproliferative activities in the low micromolar range. Finally, the highly enhanced inhibitory activities of derivative **3d**, compared with compound **A**, could be interpreted based on the results of a molecular docking study, pointing out that due to a repulsive effect between the bromine atom at the C-6 position and the oxygen of the Glu121 backbone carbonyl, additional binding interactions between Pim-1 and compound **3d** could be envisaged.

5. Experimental

5.1. In vitro kinase inhibition assays

The procedures for the in vitro protein kinase assays and for the expression and activation of the protein kinases have been detailed previously.[20]

5.1.1. Source and purification of kinases

All protein kinases were of human origin and encoded full-length proteins. All proteins were either expressed as GST (glutathione transferase) fusion proteins in *Escherichia coli* or as hexahistidine (His_6)-tagged proteins in Sf21 (*Spodoptera frugiperda* 21) insect cells. GST fusion proteins were purified by affinity chromatography on glutathione–Sepharose, and His_6-tagged proteins on nickel/nitrilotriacetate–agarose.

5.1.2. Protein kinase assays

All assays (25.5 μl volume) were carried out robotically at room temperature (21 °C) and were linear with respect to time and enzyme concentration under the conditions used. Assays were performed for 30 min using Multidrop Micro reagent dispensers (Thermo Electron Corporation, Waltham, MA, USA) in a 96-well format. The concentration of magnesium acetate in the assays was 10 mM and [γ-^{33}P]ATP (800 cpm/pmol) was used at 5 μM for Pim-2 and 20 μM for Pim-1 and Pim-3, in order to be at or below the K_m for ATP for each enzyme.

The assays were initiated with Mg–ATP, stopped by the addition of 5 μl of 0.5 M orthophosphoric acid and spotted on to P81 filter plates using a unifilter harvester (PerkinElmer, Boston, MA, USA). Kinase substrates was RSRHSSYPAGT (300 μM) for Pim-1, Pim-2, and Pim-3. The enzymes were diluted in a buffer consisting of 50 mM Tris/HCl, pH 7.5, 0.1 mM EGTA, 1 mg/mL BSA, and 0.1% 2-mercaptoethanol and assayed in a buffer comprising 50 mM Tris/HCl, pH 7.5, 0.1 mM EGTA and 0.1% 2-mercaptoethanol.

The inhibition profile of the tested compounds was expressed as the percentage of the residual kinase activity for an inhibitor concentration of 1 or 10 μM. The IC_{50} values of inhibitors were determined after carrying out assays at 10 different concentrations of each compound.

5.2. In vitro antiproliferative assays

5.2.1. Cell cultures

Stock cell cultures were maintained as monolayers in 75 cm^2 culture flasks in Glutamax Eagle's minimum essential medium (MEM) with Earle's salts supplemented with 10% fetal calf serum, 5 ml 100 mmol/l sodium pyruvate, 5 ml of 100× non-essential amino acids and 2 mg gentamicin base. Cells were grown at 37 °C in a humidified incubator under an atmosphere containing 5% CO_2.

5.2.2. Survival assays

Cells were plated at a density of 5×10^3 cells in 150 μl culture medium in each well of 96-well microplates and were allowed to adhere for 16 h before treatment with tested drug. A stock solution 20 mmol/l of each tested drug was prepared in DMSO and kept at −20 °C until use. Then 50 μl of each tested solution were added to the cultures. A 48 h continuous drug exposure protocol was used. The antiproliferative effect of the tested drug was assessed by the resazurin reduction test.

5.2.3. Resazurin reduction test

Plates were rinsed with 200 μl PBS at 37 °C and emptied by overturning on absorbent toweling. Then 150 μl of a 25 μg/ml solution of resazurin in MEM without phenol red was added to each well. Plates were incubated for 1 h at 37 °C in a humidified atmosphere containing 5% CO_2. Fluorescence was then measured on an automated 96-well plate reader (Fluoroscan Ascent FL, Labsystem) using an excitation wavelength of 530 nm and an emission wavelength of 590 nm. Under the conditions used, fluorescence was proportional to the number of living cells in the well. The IC_{50}, defined as the drug concentration required to inhibit cell proliferation by 50%, was calculated from the curve of concentration-dependent survival percentage, defined as fluorescence in experimental wells compared with fluorescence in control wells, after subtraction of the blank values.

5.3. Chemistry

IR spectra were recorded on a Shimadzu FTIR-8400S spectrometer ($\bar{\nu}$ in cm^{-1}). NMR spectra were performed on a Bruker AVANCE 400 (^{1}H: 400 MHz, ^{13}C: 100 MHz), chemical shifts δ in ppm, the following abbreviations are used: singlet (s), doublet (d), triplet (t), quadruplet (q), doublet of doublet (dd), doublet of triplet (dt), doublet of doublet of doublet (ddd), multiplet (m), broad signal (br s). Mass spectra (ESI+) were determined on a high-resolution Micro Q-Tof apparatus (CRMP, Université Blaise Pascal, Clermont-Ferrand, France) or on a Waters Q-Tof 2 apparatus (CRMPO, Université de Rennes, France). Chromatographic purifications were performed by flash Silica Gel Geduran SI 60 (Merck) 0.040–0.063 mm column chromatography. Reactions were monitored by TLC using fluorescent silica gel plates (60 F254 from Merck). Experiments under microwave irradiation were performed using a CEM Discover Benchmate apparatus. Melting points were measured on a Reichert microscope and are uncorrected. The purity of compounds was assessed by single spot TLC and NMR analysis.

5.3.1. General procedure for the preparation of compounds of examples (2a–2j)

The ionic liquid used for this step was prepared as follow: a mixture of choline chloride (10.0 g, 71.6 mmol) and zinc chloride (19.5 g, 143 mmol) in toluene (200 mL) was refluxed in a Dean–Stark apparatus under vigorous stirring for 15 h. After cooling and decantation, the ionic liquid was obtained as a yellow oil which can be directly used or conserved under inert atmosphere in anhydrous ether.

Step A: a suspension of substituted phenylhydrazine hydrochloride and anhydrous sodium acetate in DME (20 mL) was stirred at room temperature for 1 h. Compound **1** (1.10 g, 4.0 mmol) and ionic liquid (11.54 g, 28 mmol) were added. The solvent was evaporated and the mixture was stirred at 120 °C for 12 h. After cooling, a 0.5 M aqueous HCl solution was added before extraction with EtOAc. The organic fractions were washed with brine, dried over

$MgSO_4$ and filtered. This solution contained the desired product and was used directly for the oxidation step.

Step B: DDQ was added to this solution and the reaction mixture was stirred at room temperature overnight. The mixture was washed with brine, dried over $MgSO_4$, filtered and then concentrated under vacuum.

Step C: the crude mixture was dissolved in methanol (100 mL), a 5 M aqueous KOH solution (25 mL) was added and the mixture was refluxed for 12 h. After cooling, the solvent was removed under vacuum. The residue was neutralized by addition of a concentrated HCl solution. After extraction with EtOAc, the assembled organic fractions were washed with brine, dried over $MgSO_4$ and evaporated. The solid was purified by flash chromatography.

5.3.1.1. 6,8-Dichloro-1,10-dihydropyrrolo[2,3-*a*]carbazole (2a).

Step A: 3,5-dichlorophenylhydrazine hydrochloride (1.00 g, 4.68 mmol), sodium acetate (384 mg, 4.68 mmol); *step B:* DDQ (908 mg, 4.00 mmol); *step C:* flash chromatography (cyclohexane/EtOAc, from 9:1 to 7:3) provided **2a** (971 mg, 3.53 mmol, 88%) as a gray solid. Mp >250 °C; HRMS (ESI+) calcd for $C_{14}H_9{}^{35}Cl_2N_2$ $(M+H)^+$ 275.0143, found 275.0135; IR (ATR): 3431, 3368, 1653, 1616 cm^{-1}; ^1H NMR (400 MHz, DMSO-d_6): 6.62 (1H, dd, J_1 = 3,0 Hz, J_2 = 2,0 Hz), 7.27 (1H, d, J = 1.5 Hz), 7.44 (1H, dd, J_1 = 8.5 Hz, J_2 = 0.5 Hz), 7.46 (1H, dd, J_1 = 3.0 Hz, J_2 = 2.5 Hz), 7.76 (1H, d, J = 1.5 Hz), 8.05 (1H, d, J = 8.5 Hz), 11.00 (1H, br s, NH), 11.42 (1H, br s, NH); ^{13}C NMR (100 MHz, DMSO-d_6): 102.9, 110.2, 113.3, 113.4, 118.9, 124.7 (CH), 114.4, 120.0, 121.2, 126.3, 126.9, 127.3, 127.5, 139.5 (C).

5.3.1.2. 7-Fluoro-1,10-dihydropyrrolo[2,3-*a*]carbazole (2b).

Step A: 4-fluorophenylhydrazine hydrochloride (1.30 g, 8.0 mmol), sodium acetate (656 mg, 8.0 mmol); *step B:* DDQ (545 mg, 2.40 mmol); *step C:* flash chromatography (cyclohexane/EtOAc, from 9:1 to 7:3) provided **2b** (702 mg, 3.13 mmol, 78%) as a gray-green solid. Mp >250 °C; HRMS (ESI+) calcd for $C_{14}H_{10}FN_2$ $(M+H)^+$ 225.0828, found 225.0815; IR (ATR): 3418, 3387, 1645, 1584 cm^{-1}; ^1H NMR (400 MHz, DMSO-d_6): 6.58 (1H, dd, J_1 = 3.0 Hz, J_2 = 2.0 Hz), 7.12 (1H, ddd, J_1 = 9.5 Hz, J_2 = 9.0 Hz, J_3 = 2.5 Hz), 7.34 (1H, d, J = 8.5 Hz), 7.39 (1H, t, J = 2.5 Hz), 7.60 (1H, dd, J_1 = 8.5 Hz, J_2 = 4.5 Hz), 7.71 (1H, d, J = 8.5 Hz), 7.84 (1H, dd, J_1 = 9.5 Hz, J_2 = 2.5 Hz), 10.89 (1H, br s, NH), 10.92 (1H, br s, NH); ^{13}C NMR (100 MHz, DMSO-d_6): 102.9, 104.5 (d, J_{CF} = 24 Hz), 110.7 (d, J_{CF} = 25 Hz), 112.0 (d, J_{CF} = 9 Hz), 112.2 (2C), 123.9 (CH), 116.0 (d, J_{CF} = 4 Hz), 121.6, 124.6 (d, J_{CF} = 10 Hz), 126.5, 127.8, 134.6, 156.7 (d, J_{CF} = 232) (C).

5.3.1.3. 9-Fluoro-1,10-dihydropyrrolo[2,3-*a*]carbazole (2c).

Step A: 2-fluorophenylhydrazine hydrochloride (1.00 g, 6.15 mmol), sodium acetate (505 mg, 6.16 mmol); *step B:* DDQ (450 mg, 1.98 mmol); *step C:* flash chromatography (cyclohexane/EtOAc, from 9:1 to 7:3) provided **2c** (495 mg, 2.21 mmol, 55%) as beige solid. Mp >250 °C; HRMS (ESI+) calcd for $C_{14}H_{10}FN_2$ $(M+H)^+$ 225.0828, found 225.0832; IR (ATR): 3424, 3376, 1651, 1578 cm^{-1}; ^1H NMR (400 MHz, DMSO-d_6): 6.60 (1H, dd, J_1 = 3.0 Hz, J_2 = 2.0 Hz), 7.08–7.19 (2H, m), 7.39 (1H, d, J = 8.5 Hz), 7.42 (1H, t, J = 2.5 Hz), 7.73 (1H, d, J = 8.5 Hz), 7.88 (1H, d, J = 7.5 Hz), 10.61 (1H, br s, NH), 11.40 (1H, br s, NH); ^{13}C NMR (100 MHz, DMSO-d_6): 102.9, 108.6 (d, J_{CF} = 16 Hz), 112.1, 112.9, 115.3 (d, J_{CF} = 3 Hz), 119.0 (d, J_{CF} = 6 Hz), 124.1 (CH), 116.2 (d, J_{CF} = 2.5 Hz), 121.7, 125.5 (d, J_{CF} = 13 Hz), 126.7, 126.9, 128.0 (d, J_{CF} = 6 Hz), 148.9 (d, J_{CF} = 241 Hz) (C).

5.3.1.4. 6-Bromo-1,10-dihydropyrrolo[2,3-*a*]carbazole (2d) and 8-bromo-1,10-dihydropyrrolo[2,3-*a*]carbazole (2e).

Step A: 3-bromophenylhydrazine hydrochloride (1.00 g, 4.47 mmol), sodium acetate (367 mg, 4.47 mmol); *step B:* DDQ (454 mg, 2.00 mmol); *step C:* flash chromatography (cyclohexane/EtOAc, 9:1 then 8:2) provided compounds **2d** (342 mg, 1.20 mmol, 30%) and **2e** (513 mg, 1.80 mmol, 45%) as gray solids.

Compound **2d**: Mp = 249–251 °C; HRMS (ESI+) calcd for $C_{14}H_{10}{}^{79}BrN_2$ $(M+H)^+$ 285.0027, found 285.0019; IR (ATR): 3406, 3364, 1653, 1613 cm^{-1}; ^1H NMR (400 MHz, DMSO-d_6): 6.62 (1H, dd, J_1 = 3.0 Hz, J_2 = 2.0 Hz), 7.23 (1H, t, J = 8.0 Hz), 7.35 (1H, dd, J_1 = 7.5 Hz, J_2 = 0.5 Hz), 7.42 (1H, d, J = 8.5 Hz), 7.44 (1H, t, J = 2.5 Hz), 7.66 (1H, dd, J_1 = 8.0 Hz, J_2 = 0.5 Hz), 8.24 (1H, d, J = 8.5 Hz), 10.90 (1H, br s, NH), 11.31 (1H, br s, NH); ^{13}C NMR (100 MHz, DMSO-d_6): 102.8, 110.6, 112.3, 113.4, 122.5, 124.3, 124.4 (CH), 114.2, 115.4, 121.4, 122.4, 126.6, 127.0, 139.4 (C).

Compound **2e**: Mp >250 °C; HRMS (ESI+) calcd for $C_{14}H_9{}^{79}BrN_2$ $(M)^+$ 283.9949, found 285.9946; IR (ATR): 3397, 1649, 1607 cm^{-1}; ^1H NMR (400 MHz, DMSO-d_6): 6.59 (1H, dd, J_1 = 3.0 Hz, J_2 = 2.0 Hz), 7.27 (1H, dd, J_1 = 8.5 Hz, J_2 = 2.0 Hz), 7.37 (1H, dd, J_1 = 8.5 Hz, J_2 = 0.5 Hz), 7.40 (1H, dd, J_1 = 3.0 Hz, J_2 = 2.5 Hz), 7.71 (1H, dd, J_1 = 8.5 Hz, J_2 = 0.5 Hz), 7.85 (1H, dd, J_1 = 2.0 Hz, J_2 = 0.5 Hz), 7.99 (1H, d, J = 8.5 Hz), 10.94 (1H, br s, NH), 11.01 (1H, br s, NH); ^{13}C NMR (100 MHz, DMSO-d_6): 102.9, 111.9, 112.7, 113.9, 120.7, 121.3, 124.0 (CH), 115.6, 115.8, 121.6, 123.3, 126.6, 126.7, 139.1 (C).

5.3.1.5. 9-Bromo-1,10-dihydropyrrolo[2,3-*a*]carbazole (2f).

Step A: 2-bromophenylhydrazine hydrochloride (1.00 g, 4.47 mmol), sodium acetate (367 mg, 4.47 mmol); *step B:* DDQ (636 mg, 2.80 mmol); *step C:* flash chromatography (cyclohexane/EtOAc, from 9:1 to 7:3) provided **2f** (780 mg, 2.74 mmol, 68%) as a white solid. Mp >250 °C; HRMS (ESI+) calcd for $C_{14}H_{10}{}^{79}BrN_2$ $(M+H)^+$ 285.0027, found 285.0012; IR (ATR): 3314, 1636, 1622 cm^{-1}; ^1H NMR (400 MHz, DMSO-d_6): 6.60 (1H, dd, J_1 = 3.0 Hz, J_2 = 2.0 Hz), 7.11 (1H, t, J = 7.5 Hz), 7.40 (1H, dd, J_1 = 8.5 Hz, J_2 = 0.5 Hz), 7.45 (1H, dd, J_1 = 3.0 Hz, J_2 = 2.5 Hz), 7.52 (1H, dd, J_1 = 7.5 Hz, J_2 = 1.0 Hz), 7.73 (1H, dd, J_1 = 8.5 Hz, J_2 = 0.5 Hz), 8.07 (1H, dt, J_1 = 7.5 Hz, J_2 = 0.5 Hz), 10.79 (1H, br s, NH), 11.12 (1H, br s, NH); ^{13}C NMR (100 MHz, DMSO-d_6): 103.0, 112.3, 113.2, 118.6, 120.3, 124.2, 125.7 (CH), 103.6, 116.4, 121.7, 125.9, 126.5, 126.7, 136.5 (C).

5.3.1.6. 7-Nitro-1,10-dihydropyrrolo[2,3-*a*]carbazole (2g).

Step A: 4-nitrophenylhydrazine hydrochloride (1.52 g, 8.0 mmol), sodium acetate (656 mg, 8.0 mmol); *step B:* DDQ (545 mg, 2.40 mmol); *step C:* flash chromatography (cyclohexane/EtOAc, from 9:1 to 3:7) provided **2g** (450 mg, 1.79 mmol, 45%) as a yellow-brown solid. Mp = 220 °C (decomp.); HRMS (ESI+) calcd for $C_{14}H_{10}N_3O_2$ $(M+H)^+$ 252.0773, found 252.0763; IR (ATR): 3406, 3298, 1655, 1616 cm^{-1}; ^1H NMR (400 MHz, DMSO-d_6): 6.64 (1H, dd, J_1 = 3.0 Hz, J_2 = 2.0 Hz), 7.46–7.49 (2H, m), 7.79 (1H, d, J = 9.0 Hz), 7.93 (1H, d, J = 8.5 Hz), 8.22 (1H, dd, J_1 = 9.0 Hz, J_2 = 2.5 Hz), 9.06 (1H, d, J = 2.5 Hz), 11,00 (1H, br s, NH), 11,74 (1H, br s, NH); ^{13}C NMR (100 MHz, DMSO-d_6): 103.1, 111.4, 112.4, 113.9, 115.9, 119.1, 124.8 (CH), 116.3, 121.5, 123.9, 127.6, 127.9, 140.0, 141.7 (CH).

5.3.1.7. 1,10-Dihydropyrrolo[2,3-*a*]carbazole-7-carbonitrile (2h).

Step A: 4-cyanophenylhydrazine hydrochloride (1.36 g, 8.0 mmol), sodium acetate (656 mg, 8.0 mmol); *step B:* DDQ (545 mg, 2.40 mmol); *step C:* flash chromatography (cyclohexane/EtOAc, from 9:1 to 7:3) provided **2h** (517 mg, 2.24 mmol, 56%) as a beige solid. Mp >250 °C; HRMS (ESI+) calcd for $C_{15}H_{10}N_3$ $(M+H)^+$ 232.0875, found 232.0872; IR (ATR): 3439, 3256, 2226, 1655, 1614 cm^{-1}; ^1H NMR (400 MHz, DMSO-d_6): 6.63 (1H, dd, J_1 = 3.0 Hz, J_2 = 2.0 Hz), 7.42–7.46 (2H, m), 7.67 (1H, dd, J_1 = 8.5 Hz, J_2 = 1.5 Hz), 7.78 (1H, dd, J_1 = 8.5 Hz, J_2 = 0.5 Hz), 7.83 (1H, d, J = 8.5 Hz), 8.61 (1H, m), 10.97 (1H, br s, NH), 11.53 (1H, br s, NH); ^{13}C NMR (100 MHz, DMSO-d_6): 103.0, 112.2, 112.3, 113.5, 124.2, 124.6, 126.5 (CH), 100.3, 115.4, 120.9, 121.4, 124.3, 127.2, 127.3, 140.1 (C).

5.3.1.8. 9-Ethyl-1,10-dihydropyrrolo[2,3-*a*]carbazole (2i). *Step A:* 2-ethylphenylhydrazine hydrochloride (1.00 g, 5.79 mmol), sodium acetate (475 mg, 5.79 mmol); *step B:* DDQ (454 mg, 2.00 mmol); *step C:* flash chromatography (cyclohexane/EtOAc, from 9:1 to 7:3) provided **2i** (490 mg, 2.09 mmol, 52%) as a gray solid. Mp = 256–258 °C; HRMS (ESI+) calcd for $C_{16}H_{15}N_2$ $(M+H)^+$ 235.1235, found 235.1228; IR (ATR): 3426, 3416, 1649 cm^{-1}; ^1H NMR (400 MHz, DMSO-d_6): 1.40 (3H, t, J = 7.5 Hz), 2.99 (2H, q, J = 7.5 Hz), 6.57 (1H, dd, J_1 = 3.0 Hz, J_2 = 2.0 Hz), 7.09 (1H, t, J = 7.5 Hz), 7.13–7.16 (1H, m), 7.33 (1H, dd, J_1 = 8.5 Hz, J_2 = 0.5 Hz), 7.40 (1H, dd, J_1 = 3.0 Hz, J_2 = 2.5 Hz), 7.69 (1H, d, J_1 = 8.5 Hz, J_2 = 0.5 Hz), 7.87 (1H, d, J = 7.5 Hz), 10.59 (1H, br s, NH), 10.85 (1H, br s, NH); ^{13}C NMR (100 MHz, DMSO-d_6): 14.2 (CH_3), 24.1 (CH_2), 102.8, 112.1 (2C), 116.9, 118.9, 122.2, 123.5 (CH), 116.5, 121.9, 123.8, 126.0 (2C), 126.3, 136.6 (C).

5.3.1.9. 8-Methyl-1,10-dihydropyrrolo[2,3-*a*]carbazole (2j). *Step A: A* mixture of 3-methylphenylhydrazine (1.00 g, 8.2 mmol), compound **1** (1.65 g, 6.0 mmol) and ionic liquid (11.54 g, 28 mmol) was stirred at 120 °C for 12 h. After cooling, a 0.5 M aqueous HCl solution was added before extraction with EtOAc. The organic fractions were washed with brine, dried over $MgSO_4$ and filtered. This solution contained the desired product and was used directly for the oxidation step. Steps B and C were carried out as described for the preparation of compounds **2a**–**2i**; *step B*: DDQ (953 mg, 4.20 mmol); *step C:* flash chromatography (cyclohexane/EtOAc, from 9:1 to 7:3) provided **2j** (860 mg, 3.90 mmol, 65%) as a gray solid. Mp >250 °C; HRMS (ESI+) calcd for $C_{15}H_{13}N_2$ $(M+H)^+$ 221.1079, found 221.1073; IR (ATR): 3410, 3387, 1649, 1622 cm^{-1}; ^1H NMR (400 MHz, DMSO-d_6): 2.48 (3H, s), 6.55 (1H, dd, J_1 = 3.0 Hz, J_2 = 2.0 Hz), 6.95–6.98 (1H, m), 7.30 (1H, d, J = 8.5 Hz), 7.35 (1H, t, J = 2.5 Hz), 7.39 (1H, m), 7.65 (1H, d, J = 8.5 Hz), 7.89 (1H, d, J = 8.0 Hz), 10.73 (1H, br s, NH), 10.76 (1H, br s, NH); ^{13}C NMR (100 MHz, DMSO-d_6): 21.6 (CH_3), 102.7, 111.2, 111.8, 111.9, 118.8, 120.1, 123.4 (CH), 116.2, 121.9 (2C), 125.9, 126.2, 132.6, 138.6 (C).

5.3.2. General procedure for the preparation of compounds of examples (3a–3j)

$POCl_3$ (3 equiv) was slowly added to anhydrous DMF (2 mL) at 0 °C. The solution was stirred at room temperature for 45 min until a yellow solution was obtained, and then was added to a solution of compounds **2a–2j** (100 mg) in DMF (1 mL) at 0 °C prepared in a 10 mL CEM reaction vessel. The tube was sealed and was heated at 100 °C under microwave irradiation for 20 min (150 W). After cooling, the mixture was poured into a saturated aqueous $NaHCO_3$ solution (20 mL). After 30 min of stirring, the solid was filtered off and a 5% aqueous NaOH solution (20 mL) was added. The mixture was stirred at room temperature overnight. The solid was filtered off and then purified by flash chromatography.

5.3.2.1. 6,8-Dichloro-1,10-dihydropyrrolo[2,3-*a*]carbazole-3-carbaldehyde (3a). Flash chromatography (cyclohexane/EtOAc, from 3:7 to 1:9) provided **3a** (52 mg, 0.172 mmol, 47%) as a brown solid. Mp >250 °C; HRMS (ESI+) calcd for $C_{15}H_9{}^{35}Cl_2N_2O$ $(M+H)^+$ 303.0092, found 303.0073; IR (ATR): 3352, 1717, 1630 cm^{-1}; ^1H NMR (400 MHz, DMSO-d_6): 7.34 (1H, d, J = 1.5 Hz), 7.84 (1H, d, J = 1.5 Hz), 8.01 (1H, d, J = 8.5 Hz), 8.27 (1H, d, J = 8.5 Hz), 8.36 (1H, d, J = 3.0 Hz), 10.05 (1H, s, C*H*O), 11.54 (1H, br s, NH), 11.99 (1H, br s, NH); ^{13}C NMR (100 MHz, DMSO-d_6): 110.5, 113.2, 116.4, 119.3, 137.4 (CH), 116.5, 119.4, 119.5, 122.3, 123.2, 126.7, 126.9, 128.4, 139.8 (C), 185.4 (C=O).

5.3.2.2. 7-Fluoro-1,10-dihydropyrrolo[2,3-*a*]carbazole-3-carbaldehyde (3b). Flash chromatography (cyclohexane/EtOAc, from 3:7 to 1:9) provided **3b** (96 mg, 0.381 mmol, 85%) as a brown solid. Mp >250 °C; HRMS (ESI+) calcd for $C_{15}H_{10}FN_2O$ $(M+H)^+$ 253.0777, found 253.0773; IR (ATR): 3314, 1636, 1622 cm^{-1}; ^1H NMR (400 MHz, DMSO-d_6): 7.20 (1H, ddd, J_1 = 9.5 Hz, J_2 = 9.0 Hz, J_3 = 2.5 Hz), 7.67 (1H, dd, J_1 = 9.0 Hz, J_2 = 4.5 Hz), 7.91 (1H, d, J = 8.5 Hz), 7.92–7.95 (1H, m), 7.96 (1H, d, J = 8.5 Hz), 8.30 (1H, d, J = 3.0 Hz), 10.03 (1H, s, C*H*O), 11.07 (1H, br s, NH), 11.92 (1H, br s, NH); ^{13}C NMR (100 MHz, DMSO-d_6): 105.0 (d, J_{CF} = 24 Hz), 111.8 (d, J_{CF} = 25 Hz), 112.2, 112.4 (d, J_{CF} = 9 Hz), 115.4, 136.8 (CH), 118.2 (d, J_{CF} = 4 Hz), 119.6, 122.7, 122.9, 124.1 (d, J_{CF} = 10 Hz), 127.3, 135.0, 156.8 (d, J_{CF} = 232 Hz) (C), 185.4 (C=O).

5.3.2.3. 9-Fluoro-1,10-dihydropyrrolo[2,3-*a*]carbazole-3-carbaldehyde (3c). Flash chromatography (cyclohexane/EtOAc, from 8:2 to 3:7) provided **3c** (80 mg, 0.317 mmol, 71%) as a brown solid. Mp >250 °C; HRMS (ESI+) calcd for $C_{15}H_{10}FN_2O$ $(M+H)^+$ 253.0777, found 253.0792; IR (ATR): 3450–3120, 1624 cm^{-1}; ^1H NMR (400 MHz, DMSO-d_6): 7.17 (1H, dt, J_1 = 5.0 Hz, J_2 = 8.0 Hz), 7.24 (1H, ddd, J_1 = 11.0 Hz, J_2 = 8.0 Hz, J_3 = 1.0 Hz), 7.94–7.97 (2H, m), 7.98 (1H, d, J = 8.5 Hz), 8.31 (1H, d, J = 3.0 Hz), 10.05 (1H, s, C*H*O), 11.52 (1H, br s, NH), 11.57 (1H, br s, NH); ^{13}C NMR (100 MHz, DMSO-d_6): 109.4 (d, J_{CF} = 16 Hz), 112.9, 115.2, 115.8 (d, J_{CF} = 3 Hz), 119.5 (d, J_{CF} = 6 Hz), 137.1 (CH), 118.3 (d, J_{CF} = 2.5 Hz), 119.5, 122.8, 123.0, 125.9 (d, J_{CF} = 13 Hz), 126.4, 127.4 (d, J_{CF} = 6 Hz), 148.9 (d, J_{CF} = 241 Hz) (C), 185.5 (C=O).

5.3.2.4. 6-Bromo-1,10-dihydropyrrolo[2,3-*a*]carbazole-3-carbaldehyde (3d). Flash chromatography (cyclohexane/EtOAc, from 7:3 to 1:9) provided **3d** (55 mg, 0.176 mmol, 50%) as a brown solid. Mp >250 °C; HRMS (ESI+) calcd for $C_{15}H_9{}^{79}BrN_2NaO$ $(M+Na)^+$ 334.9796, found 334.9794; IR (ATR): 3300, 1620 cm^{-1}; ^1H NMR (400 MHz, DMSO-d_6): 7.30 (1H, t, J = 8.0 Hz), 7.41 (1H, d, J = 7.5 Hz), 7.73 (1H, d, J = 8.0 Hz), 7.99 (1H, d, J = 8.5 Hz), 8.34 (1H, d, J = 3.0 Hz), 8.46 (1H, d, J = 8.5 Hz), 10.05 (1H, s, C*H*O), 11.46 (1H, br s, NH), 11.91 (1H, br s, NH); ^{13}C NMR (100 MHz, DMSO-d_6): 111.0, 112.3, 116.3, 123.0, 125.2, 137.3 (CH), 114.6, 117.5, 119.5, 121.8, 122.4, 122.9, 126.6, 139.8 (C), 185.4 (C=O).

5.3.2.5. 8-Bromo-1,10-dihydropyrrolo[2,3-*a*]carbazole-3-carbaldehyde (3e). Flash chromatography (cyclohexane/EtOAc, from 7:3 to 1:9) provided **3e** (66 mg, 0.21 mmol, 60%) as a brown solid. Mp >250 °C; HRMS (ESI+) calcd for $C_{15}H_{10}{}^{79}BrN_2O$ $(M+H)^+$ 312.9976, found 312.9985; IR (ATR): 3393, 3330–3160, 1624 cm^{-1}; ^1H NMR (400 MHz, DMSO-d_6): 7.33 (1H, dd, J_1 = 8.5 Hz, J_2 = 2.0 Hz), 7.93 (1H, d, J = 1.5 Hz), 7.94 (1H, d, J = 8.5 Hz), 7.97 (1H, d, J = 8.5 Hz), 8.07 (1H, d, J = 8.5 Hz), 8.31 (1H, d, J = 3.0 Hz), 10.03 (1H, s, C*H*O), 11.13 (1H, br s, NH), 11.96 (1H, br s, NH); ^{13}C NMR (100 MHz, DMSO-d_6): 112.7, 114.3, 115.1, 121.2, 121.8, 137.0 (CH), 116.8, 117.8, 119.5, 122.6, 122.7, 123.0, 126.3, 139.4 (C), 185.4 (C=O).

5.3.2.6. 9-Bromo-1,10-dihydropyrrolo[2,3-*a*]carbazole-3-carbaldehyde (3f). Flash chromatography (cyclohexane/EtOAc, from 7:3 to 1:9) provided **3f** (90 mg, 0.287 mmol, 82%) as a brown solid. Mp >250 °C; HRMS (ESI+) calcd for $C_{15}H_{10}{}^{79}BrN_2O$ $(M+H)^+$ 312.9976, found 312.9991; IR (ATR): 3400–3100, 1630 cm^{-1}; ^1H NMR (400 MHz, DMSO-d_6): 7.16 (1H, t, J = 7.5 Hz), 7.59 (1H, dd, J_1 = 7.5 Hz, J_2 = 1.0 Hz), 7.98 (2H, s), 8.15 (1H, d, J = 7.5 Hz), 8.34 (1H, d, J = 3.0 Hz), 10.05 (1H, s, C*H*O), 11.27 (1H, br s, NH), 11.69 (1H, br s, NH); ^{13}C NMR (100 MHz, DMSO-d_6): 113.1, 115.4, 119.1, 120.6, 126.5, 137.1 (CH), 103.8, 118.5, 119.5, 122.7, 123.0, 125.2, 126.0, 136.7 (C), 185.5 (C=O).

5.3.2.7. 7-Nitro-1,10-dihydropyrrolo[2,3-*a*]carbazole-3-carbaldehyde (3g). Flash chromatography (cyclohexane/EtOAc, from 3:7 to 1:9) provided **3g** (39 mg, 0.14 mmol, 35%) as a yellow-brown solid. Mp >250 °C; HRMS (ESI+) calcd for $C_{15}H_{10}N_3O_3$ $(M+H)^+$ 280.0722, found 280.0714; IR (ATR): 3350–3150, 1636, 1614 cm^{-1}; ^1H NMR (400 MHz, DMSO-d_6): 7.85 (1H, d, J = 9.0 Hz),

8.04 (1H, d, J = 8.5 Hz), 8.19 (1H, d, J = 8.5 Hz), 8.28 (1H, dd, J_1 = 9.0 Hz, J_2 = 2.5 Hz), 8.37 (1H, d, J = 2.5 Hz), 9.14 (1H, d, J = 2.0 Hz), 10.06 (1H, s, C*H*O), 11.87 (1H, br s, NH), 12.03 (1H, br s, NH); ^{13}C NMR (100 MHz, DMSO-d_6): 111.8, 113.8, 115.7, 116.5, 119.9, 137.5 (CH), 118.4 119.5, 122.6, 123.3, 123.9, 127.5, 140.3, 142.0 (C), 185.5 (C=O).

5.3.2.8. 3-Formyl-1,10-dihydropyrrolo[2,3-*a*]carbazole-7-carbonitrile (3h). Flash chromatography (cyclohexane/EtOAc, from 3:7 to 1:9) provided **3h** (58.3 mg, 0.225 mmol, 52%) as a brown solid. Mp >250 °C; HRMS (ESI+) calcd for $C_{16}H_{10}N_3O$ $(M+H)^+$ 260.0824, found 260.0833; IR (ATR): 3287, 3239, 2212, 1630, 1618 cm^{-1}; ^{1}H NMR (400 MHz, DMSO-d_6): 7.74 (1H, dd, J_1 = 8.5 Hz, J_2 = 1.5 Hz), 7.85 (1H, dd, J_1 = 8.5 Hz, J_2 = 0.5 Hz), 8.01 (1H, d, J = 8.5 Hz), 8.08 (1H, d, J = 8.5 Hz), 8.35 (1H, d, J = 3.0 Hz), 8.70 (1H, d, J = 1.5 Hz), 10.05 (1H, s, C*H*O), 11.65 (1H, br s, NH), 11.97 (1H, br s, NH); ^{13}C NMR (100 MHz, DMSO-d_6): 112.7, 113.4, 115.4, 124.8, 127.3, 137.3 (CH), 100.8, 117.6, 119.5, 120.6, 122.5, 123.6, 123.7, 126.8, 140.5 (C), 185.5 (C=O).

5.3.2.9. 9-Ethyl-1,10-dihydropyrrolo[2,3-*a*]carbazole-3-carbaldehyde (3i). Flash chromatography (cyclohexane/EtOAc, from 8:2 to 3:7) provided **3i** (56 mg, 0.213 mmol, 50%) as a brown solid. Mp >250 °C; HRMS (ESI+) calcd for $C_{17}H_{15}N_2O$ $(M+H)^+$ 263.1184, found 263.1169; IR (ATR): 3450–3150, 1626 cm^{-1}; ^{1}H NMR (400 MHz, DMSO-d_6): 1.40 (3H, t, J = 7.5 Hz), 3.00 (2H, q, J = 7.5 Hz), 7.14 (1H, t, J = 7.5 Hz), 7.20–7.23 (1H, m), 7.90 (1H, d, J = 8.5 Hz), 7.93 (1H, d, J = 8.0 Hz), 7.93–7.96 (1H, m), 8.29 (1H, d, J = 3.0 Hz), 10.03 (1H, s, C*H*O), 11.00 (1H, br s, NH), 11.54 (1H, br s, NH); ^{13}C NMR (100 MHz, DMSO-d_6): 14.1 (CH_3), 24.0 (CH_2), 112.1, 115.1, 117.3, 119.3, 123.1, 136.7 (CH), 118.7, 119.5, 122.3, 122.9, 123.2, 125.9, 126.2, 137.0 (C), 185.4 (C=O).

5.3.2.10. 8-Methyl-1,10-dihydropyrrolo[2,3-*a*]carbazole-3-carbaldehyde (3j). Flash chromatography (cyclohexane/EtOAc from 7:3 to 1:9) provided **3j** (65 mg, 0.26 mmol, 58%) as a brown solid. Mp = 250 °C (decomp.); HRMS (ESI+) calcd for $C_{16}H_{13}N_2O$ $(M+H)^+$ 249.1028, found 249.1026; IR (ATR): 3379, 3341, 1634 cm^{-1}; ^{1}H NMR (400 MHz, DMSO-d_6): 2.49 (3H, s), 7.02 (1H, d, J = 8.0 Hz), 7.46 (1H, s), 7.89 (2H, s), 7.97 (1H, d, J = 8.0 Hz), 8.27 (1H, d, J = 3.0 Hz), 10.02 (1H, s, C*H*O), 11.88 (1H, br s, NH), 11.81 (1H, br s, NH); ^{13}C NMR (100 MHz, DMSO-d_6): 21.6 (CH_3), 111.5, 112.0, 114.8, 119.2, 120.6, 136.8 (CH), 118.5, 119.5, 121.3, 122.2, 122.8, 125.8, 133.7, 139.0 (C), 185.3 (C=O).

5.3.3. Methyl 3-formyl-1,10-dihydropyrrolo[2,3-*a*]carbazole-9-carboxylate (3k) and 9-trifluoromethyl-1,10-dihydropyrrolo[2,3-*a*]carbazole-3-carbaldehyde (3l)

Step A: A suspension of 2-trifluoromethylphenylhydrazine hydrochloride (200 mg, 0.94 mmol) and anhydrous sodium acetate (77 mg, 0.94 mmol) in DME (20 mL) was stirred at room temperature for 1 h. Compound **1** (220 mg, 0.80 mmol) and ionic liquid (2.30 g, 5.6 mmol) were added. The solvent was evaporated and the mixture was stirred at 120 °C for 12 h. After cooling, a 0.5 M aqueous HCl solution was added before extraction with EtOAc. The organic fractions were washed with brine, dried over $MgSO_4$ and filtered. This solution contained the desired product and was used directly for the oxidation step.

Step B: MnO_2 (0.5 g) was added to this solution and the reaction mixture was refluxed overnight. After cooling, the mixture was washed with brine, dried over $MgSO_4$, filtered and then concentrated under vacuum.

Step C: the crude mixture was dissolved in methanol (50 mL), a 5 M aqueous KOH solution (10 mL) was added and the mixture was refluxed for 12 h. After cooling, the solvent was removed under vacuum. The residue was neutralized by addition of a concentrated HCl solution. After extraction with EtOAc, the assembled organic fractions were washed with brine, dried over $MgSO_4$ and evaporated. The crude was used directly for the formylation step.

Step D: $POCl_3$ (100 μl) was slowly added to anhydrous DMF (2 mL) at 0 °C. The solution was stirred at room temperature for 45 min until a yellow solution was obtained, and then was added to a solution at 0 °C of the crude mixture from step C in DMF (1 mL), prepared in a 10 mL CEM reaction vessel. The tube was sealed and was heated at 100 °C under microwave irradiation for 20 min (150 W). After cooling, the mixture was poured into a 5% aqueous $NaHCO_3$ solution (20 mL) and the mixture was stirred at room temperature overnight. The solid was filtered off and then purified by flash chromatography (cyclohexane/EtOAc, from 9:1 to 7:3) to give **3k** (20 mg, 0.068 mmol, 9%) as a beige solid and **3l** (30 mg, 0.099 mmol, 12%) as a brown solid.

Compound **3k**: Mp >250 °C; HRMS (ESI+) calcd for $C_{17}H_{13}N_2O_3$ $(M+H)^+$ 293.0926, found 293.0919; IR (ATR): 3376, 1699, 1634 cm^{-1}; ^{1}H NMR (400 MHz, DMSO-d_6): 4.03 (3H, s, CH_3), 7.32 (1H, t, J = 7.5 Hz), 7.98–8.02 (2H, m), 8.04 (1H, d, J = 8.5 Hz), 8.37 (1H, d, J = 3.0 Hz), 8.45 (1H, d, J = 7.5 Hz), 10.04 (1H, s, C*H*O), 11.65 (1H, br s, NH), 12.31 (1H, br s, NH); ^{13}C NMR (100 MHz, DMSO-d_6): 52.1 (CH_3), 113.1, 115.1, 118.7, 125.2, 125.9, 136.8 (CH), 111.8, 117.5, 119.5, 122.8, 123.2, 125.2, 126.3, 137.8 (C), 166.7, 185.4 (C=O).

Compound **3l**: Mp >250 °C; HRMS (ESI+) calcd for $C_{16}H_{10}F_3N_2O$ $(M+H)^+$ 303.0745, found 303.0738; IR (ATR): 3380–3190, 1653, 1629, 1616 cm^{-1}; ^{1}H NMR (400 MHz, DMSO-d_6): 7.38 (1H, t, J = 7.5 Hz), 7.71 (1H, d, J = 7.5 Hz), 8.01 (1H, d, J = 8.5 Hz), 8.06 (1H, d, J = 8.5 Hz), 8.36 (1H, d, J = 3.0 Hz), 8.46 (1H, d, J = 8.0 Hz), 10.06 (1H, s, CHO), 11.46 (1H, br s, NH), 11.73 (1H, br s, NH); ^{13}C NMR (100 MHz, DMSO-d_6): 113.3, 115.1, 118.8, 121.3 (q, J_{CF} = 4.5 Hz), 124.2, 137.1 (CH), 111.5 (q, J_{CF} = 32 Hz), 117.4, 119.4, 122.5, 123.3, 124.9 (q, J_{CF} = 271 Hz), 125.5, 126.4, 133.5 (q, J_{CF} = 2 Hz) (C), 185.5 (C=O).

5.4. Molecular docking

Molecular modeling and docking experiments were performed using Sybylx1.1 (Tripos Inc., St. Louis, MO),[21] and Surflex-Dock. Protein coordinates of the co-crystal structure of Pim-1 and compound **A** were taken from the Protein Data Bank (PDB code 3JPV). Hydrogen atoms were added using Sybyl and the protein structure was further prepared with Surflex-Dock. The GeomX docking option was used with Threshold set to 0.10 and Bloat set to 0. Docking performed in these conditions considered potential hydrogen bonding without taking into account electrostatic charges. Furthermore, the best result obtained for each ligand was minimized without any constraint in a volume constructed with a distance of 10 Å around the ligand and including the entire active site. These minimizations were carried out with the Tripos force field, Gasteiger-Hückel charges, dielectric constant set to 1 and conjugate gradient method. Moreover, similar results were obtained when the docking studies were performed with AutoDock4.2[24] program using Gasteiger-Hückel charges.

Acknowledgments

The authors thank Région Auvergne, PRAI e-nnovergne LifeGrid, European Union Prokinase Research Consortium and CNRS Valorisation for financial support. We are also grateful to Bertrand Légeret for mass spectrometry analysis.

References and notes

1. Grey, R.; Pierce, A. C.; Bemis, G. W.; Jacobs, M. D.; Moody, C. S.; Jajoo, R.; Mohal, N.; Green, J. *Bioorg. Med. Chem. Lett.* **2009**, *19*, 3019.

2. Morishita, D.; Katayama, R.; Sekimizu, K.; Tsuruo, T.; Fujita, N. *Cancer Res.* **2008**, *68*, 5076.
3. Bullock, A. N.; Debreczeni, J.; Amos, A. N.; Knapp, S.; Turk, B. E. *J. Biol. Chem.* **2005**, *280*, 41675.
4. Macdonald, A.; Campbell, D. G.; Toth, R.; McLauchlan, H.; Hastie, C. J.; Arthur, J. S. C. *BMC Cell Biol.* **2006**, *7*, doi:10.1186/1471-2121-7-1.
5. Tong, Y.; Steward, K. D.; Thomas, S.; Przytulinska, M.; Johnson, E. F.; Klinghofer, V.; Leverson, J.; McCall, O.; Soni, N. B.; Luo, Y.; Lin, N.-H.; Sowin, T. J.; Giranda, V. L.; Penning, T. D. *Bioorg. Med. Chem. Lett.* **2008**, *18*, 5206.
6. Cheney, I. W.; Yan, S.; Appleby, T.; Walker, H.; Vo, T.; Yao, N.; Hamatake, R.; Hong, Z.; Wu, J. Z. *Bioorg. Med. Chem. Lett.* **2007**, *17*, 1679.
7. Holder, S.; Zemskova, M.; Zhang, C.; Tabrizizad, M.; Bremer, R.; Neidligh, J. W.; Lilly, M. B. *Mol. Cancer Ther.* **2007**, *6*, 163.
8. Debreczeni, J. E.; Bullock, A. N.; Atilla, G. E.; Williams, D. S.; Bregman, H.; Knapp, S.; Meggers, E. *Angew. Chem., Int. Ed.* **2006**, *45*, 1580.
9. Xia, Z.; Knaak, C.; Ma, J.; Beharry, Z. M.; McInnes, C.; Wang, W.; Kraft, A. S.; Smith, C. D. *J. Med. Chem.* **2009**, *52*, 74.
10. Bullock, A. N.; Debreczeni, J. E.; Federov, O. Y.; Nelson, A.; Marsden, B. D.; Knapp, S. *J. Med. Chem.* **2005**, *48*, 7604.
11. Pogacic, V.; Bullock, A. N.; Federov, O.; Filippakopoulos, P.; Gasser, C.; Biondi, A.; Meyer-Monard, S.; Knapp, S.; Schwaller, J. *Cancer Res.* **2007**, *67*, 6916.
12. Pierce, A. C.; Jacobs, M.; Stuver-Moody, C. *J. Med. Chem.* **2008**, *51*, 1972.
13. Olla, S.; Manetti, F.; Crespan, E.; Maga, G.; Angelucci, A.; Schenone, S.; Bologna, M.; Botta, M. *Bioorg. Med. Chem. Lett.* **2009**, *19*, 1512.
14. Qian, K.; Wang, L.; Cywin, C. L.; Farmer, B. T., II; Hickey, E.; Homon, C.; Jakes, S.; Kashem, M. A.; Lee, G.; Leonard, S.; Li, J.; Magboo, R.; Mao, W.; Pack, E.; Peng, C., ; Prokopowicz, A., III; Welzel, M.; Wolak, J.; Morwick, T. *J. Med. Chem.* **2009**, *52*, 1814.
15. Anand, R.; Maksimoska, J.; Pagano, N.; Wong, E. Y.; Gimotty, P. A.; Diamond, S. L.; Meggers, E.; Marmorstein, R. *J. Med. Chem.* **2009**, *52*, 1602.
16. Bullock, A. N.; Debreczeni, J. E.; Fedorov, O. Y.; Nelson, A.; Marsden, B. D.; Knapp, S. *J. Med. Chem.* **2005**, *48*, 7604.
17. Akué-Gédu, R.; Rossignol, E.; Azzaro, S.; Knapp, S.; Filippakopoulos, P.; Bullock, A. N.; Bain, J.; Cohen, P.; Prudhomme, M.; Anizon, F.; Moreau, P. *J. Med. Chem.* **2009**, *52*, 6369.
18. Kakushima, M.; Hamel, P.; Frenette, R.; Rokach, J. *J. Org. Chem.* **1983**, *48*, 3214.
19. Kimoto, H.; Cohen, L. A. *J. Org. Chem.* **1980**, *45*, 3831.
20. Bain, J.; Plater, L.; Elliott, M.; Shpiro, N.; Hastie, J.; McLauchlan, H.; Klervernic, I.; Arthur, S. C.; Alessi, D. R.; Cohen, P. *Biochem. J.* **2007**, *408*, 297.
21. Sybylx1.1, Tripos International, 1699 South Hanley Rd., St. Louis, Missouri, 63144, USA.
22. Pettersen, E. F.; Goddard, T. D.; Huang, C. C.; Couch, G. S.; Greenblatt, D. M.; Meng, E. C.; Ferrin, T. E. *J. Comput. Chem.* **2004**, *25*, 1605.
23. O'Brien, J.; Wilson, I.; Orton, T.; Pognan, F. *Eur. J. Biochem.* **2000**, *267*, 5421.
24. Morris, G. M.; Goodsell, D. S.; Halliday, R. S.; Huey, R.; Hart, W. E.; Belew, R. K.; Olson, A. J. *J. Comput. Chem.* **1998**, *19*, 1639.